UC Davis
UC Davis Previously Published Works

Title

Aflatoxin B1 exposure disrupts the intestinal immune function via a soluble epoxide hydrolase-mediated manner

Permalink

https://escholarship.org/uc/item/4hg6g135

Authors

Wang, Weicang

Wang, Yuxin

Yang, Jun

et al.

Publication Date

2023

DOI

10.1016/j.ecoenv.2022.114417

Peer reviewed

Aflatoxin B₁ exposure disrupts the intestinal immune function via a soluble epoxide hydrolase-mediated manner

Weicang Wang[a,1], **Yuxin Wang**[a,1], **Jun Yang**[a,1], **Karen M. Wagner**[a], **Sung Hee Hwang**[a], **Jeff Cheng**[a], **Nalin Singh**[a], **Patricia Edwards**[b], **Christophe Morisseau**[a], **Guodong Zhang**[c], **Dipak Panigrahy**[d,e], **Bruce D. Hammock**[a,*]

[a]Department of Entomology and Nematology, and UC Davis Comprehensive Cancer Center, University of California, Davis, CA, USA

[b]Center for Health and the Environment, University of California Davis, Davis, CA, USA

[c]Department of Food Science and Technology, National University of Singapore, Singapore

[d]Department of Pathology, Beth Israel Deaconess Medical Center, Harvard Medical School, Boston, MA, USA

[e]Center for Vascular Biology Research, Beth Israel Deaconess Medical Center, Harvard Medical School, Boston, MA, USA

Abstract

Aflatoxin B₁ (AFB₁) contamination in food and feed leads to severe global health problems. Acting as the frontier immunological barrier, the intestinal mucosa is constantly challenged by exposure to foodborne toxins such as AFB₁ via contaminated diets, but the detailed toxic mechanism and endogenous regulators of AFB₁ toxicity are still unclear. Here, we showed that AFB₁ disrupted intestinal immune function by suppressing macrophages, especially M2 macrophages, and antimicrobial peptide-secreting Paneth cells. Using an oxylipinomics approach, we identified that AFB₁ immunotoxicity is associated with decreased epoxy fatty acids, notably epoxyeicosatrienoic acids, and increased soluble epoxide hydrolase (sEH) levels in the intestine. Furthermore, sEH deficiency or inhibition rescued the AFB₁-compromised intestinal immunity by restoring M2 macrophages as well as Paneth cells and their-derived lysozyme and α-defensin-3 in mice. Altogether, our study demonstrates that AFB₁ exposure impairs intestinal immunity, at least in part, in a sEH-mediated way. Moreover, the present study supports the potential application of pharmacological intervention by inhibiting the sEH enzyme in alleviating intestinal immunotoxicity and associated complications caused by AFB₁ global contamination.

Graphical abstract

---

[*]To whom correspondence should be addressed: Bruce D. Hammock, bdhammock@ucdavis.edu.
[1]W.W., Y.W. and J.Y. contributed equally to this work.
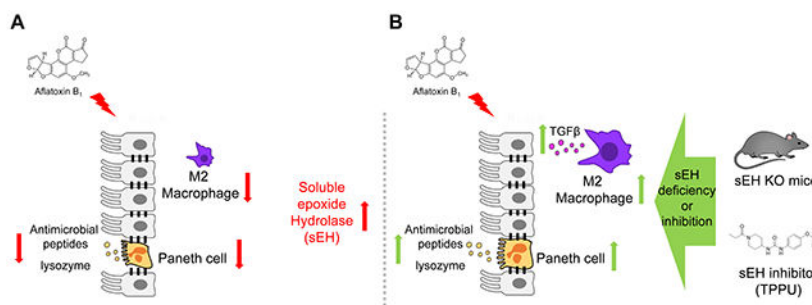
Keywords

aflatoxin B_1; intestinal immunotoxicity; soluble epoxide hydrolase; M2 macrophage; Paneth cell

1. Introduction

Aflatoxin B_1 (AFB_1) is among the most commonly occurring mycotoxins in food and feed. Approximately 4.5 billion people and millions of farm animals are at risk of exposure to AFB_1 via contaminated diets particularly in developing countries (Williams et al., 2004). Intestinal mucosa, where most AFB_1 gets absorbed and metabolized (Kumagai, 1989), is among the first barriers and largest immune systems targeted by such toxic foodborne contaminants. Previous studies showed that AFB_1 suppressed the intestinal T cells and IgA^+ cells in chicken and rodent models (Jiang et al., 2015a; Jiang et al., 2015b; Tomkova et al., 2002), although the more detailed immunotoxic effects remain to be elucidated. Impaired intestinal immune function due to AFB_1 exposure contributes to increased pathogen infection and associated diseases. Notably, dietary exposure to AFB_1 exacerbated enteropathogen *Salmonella* sp.-induced paratyphoid and *Eimeria* sp.-induced coccidiosis in chickens or quail (Boonchuvit and Hamilton, 1975; Rao et al., 1995; Ruff, 1978). Intake of AFB_1 also exaggerated erysipelas caused by the foodborne pathogen *Erysipelothrix rhusiopathiae* in pigs (Cysewski et al., 1978). In humans, aflatoxicosis is featured by severe gastrointestinal tract symptoms, including vomiting, rectal bleeding, and infection (Mwanda et al., 2005). Therefore, it is important to better understand the pathological mechanism and identify the cellular regulator, in order to develop target-based strategies to alleviate the AFB_1 intestinal immunotoxicity and associated complications.

Previous studies highlighted that AFB_1 is a membrane-active compound stimulating the arachidonic acid (ARA) detachment from the cell membrane (Amstad et al., 1984; Iida et al., 1998; Liu et al., 1990). Released ARA will further go through enzymatic metabolism pathways to generate bioactive fatty acid metabolites, termed eicosanoids (Harizi et al., 2008). There are three major enzymatic metabolism cascades that are responsible for eicosanoid biosynthesis: cyclooxygenases (COX), lipoxygenases (LOX), and cytochrome P450 (CYP) monooxygenases-soluble epoxide hydrolase (sEH) pathways. ARA, linoleic acid (LA), α-linolenic acid (ALA), eicosapentaenoic acid (EPA), docosahexaenoic acid (DHA), and other polyunsaturated fatty acids (PUFAs) are also substrates for these pathways. Accumulating evidence showed that eicosanoids and their metabolic pathways play critical roles in controlling immune function by recruiting leukocytes, activating

immune signaling, and stimulating cytokine and antibody production (Dennis and Norris, 2015; Sheppe and Edelmann, 2021; Wei and Gronert, 2019). However, whether these pathways are involved in regulating the effect of AFB$_1$ on intestinal immunity is still unknown.

To this end, we determined the effect of AFB$_1$ on intestinal immunity in a C57BL/6 mouse model. To investigate the roles of eicosanoids on AFB$_1$ immunotoxicity, we applied a quantitative oxylipinomics approach to systemically analyze more than 100 eicosanoid metabolites synthesized by COX, LOX, CYP and sEH enzymes. We found that AFB$_1$ suppressed intestinal immunity by suppressing M2 macrophages and Paneth cells, paralleled with decreased epoxy fatty acids (EpFAs) and increased sEH expression. We therefore used sEH genetic knockout mice (*Ephx2$^{-/-}$* mice) and a small-molecule inhibitor to determine the function of sEH in mediating AFB$_1$ toxicity in the intestine. Our study supports that sEH acts as a promising target for reducing or treating AFB$_1$-induced intestinal immunity defects.

2. Materials and Methods

2.1. Animal experiments

All animal experiment protocols were approved by the Institutional Animal Care and Use Committee at the University of California-Davis. C57BL/6 male mice (purchased from Charles River Laboratories) were maintained in a standard animal facility. After receipt, the mice were acclimated to the vivarium for 3 days before the study. During the study, all the mice were kept on a standard chow diet, which was always available.

Animal experiment 1: Effects of AFB$_1$ exposure on intestinal immune function —C57BL/6 male mice (8-week-old) were randomly assigned to four equal groups (n = 6 mice per group, 3 mice in a cage) and orally exposed to three different doses of AFB$_1$ or vehicle (drinking water containing 0.1% DMSO) control for 21 days. AFB$_1$ (Sigma-Aldrich, catalog # A6636) was dissolved in DMSO and added to sterile drinking water (the final concentration of DMSO is 0.1%). The final concentration of AFB$_1$ is 0.5, 1.5, or 5 mg/L, respectively. Accordingly, the estimated exposure dose of AFB$_1$ in mice is 0.06, 0.18, or 0.6 mg/kg body weight (b.w.) per day (mg·kg^{-1}·d^{-1}), respectively, calculated with the average body weight of 25 g and water intake of 3 mL/day. Both vehicle and AFB$_1$ drinking water were freshly prepared every other day, and put in aluminum foil-wrapped bottles to retard the photochemical degradation of AFB$_1$ and minimize degradation-caused dose changes. The total water intake per cage from the vehicle control or each AFB$_1$ treatment group was measured during the experiment (Fig. S1). After 21 days, the mice were euthanized to dissect the proximal part of the small intestine where the AFB$_1$ absorption and exposure are highest (Kumagai, 1989).

Animal experiment 2: Effects of genetic knockout of sEH on AFB$_1$-disrupted intestinal immune function—C57BL/6 male WT mice or *Ephx2$^{-/-}$* mice (8-week-old, n = 8 mice per group) were treated with AFB$_1$ (5 mg/L) or vehicle (drinking water containing 0.1% DMSO). As above, both vehicle and AFB$_1$ drinking water were freshly prepared every other day and put in aluminum foil-wrapped bottles. After 21 days, the mice were euthanized to dissect the proximal part of small intestine for analysis.

Animal experiment 3: Effects of sEH inhibitor on AFB₁-disrupted intestinal immune function—C57BL/6 male mice (8-week old) were randomly assigned to three equal groups (n = 6 mice per group): the first group was given vehicle (drinking water containing 0.15% DMSO); the second group was given AFB$_1$ (5 mg/L) in vehicle; and the third group was pretreated with the sEH inhibitor N-[1-(1-oxopropyl)-4-piperidinyl]-N'-[4-(trifluoromethoxy)phenyl]-urea (TPPU) at the concentration of 10mg/L in drinking water, which is a well-established delivery method to achieve the inhibitory effect of sEH action based on previous studies (Goswami et al., 2016; Jiang et al., 2020; Wang et al., 2012; Wang et al., 2020), containing 0.05% DMSO for 3 days. Then this group was continued to be given the sEH inhibitor TPPU (10 mg/L) together with the AFB$_1$ (5 mg/L) in vehicle (drinking water containing 0.15% DMSO). The dose of TPPU was chosen based on previous studies showing the efficacy for attenuating obesity-induced gut disorders under this dose (Wang et al., 2018b). Moreover, previous pharmacokinetic study showed when orally giving the mice 0.3 mg/kg TPPU, the TPPU plasma concentration reaches 495 nM (Lee et al., 2014), which is much higher than the IC$_{50}$ (2.8 nM) for murine sEH (Rose et al., 2010). All of the vehicle, AFB$_1$ only, and AFB$_1$ plus TPPU drinking water were freshly prepared every other day and kept with aluminum foil covering. After 21 days, the mice were euthanized to dissect the proximal part of the small intestine for analysis.

2.2 LC-MS/MS-based oxylipinomics analysis

The oxylipinomics analysis was conducted as previously described (Wang et al., 2018b). Briefly, the tissue from proximal small intestine (~30 mg) was dissected, mixed with the extract solution containing the antioxidant and internal standards, and homogenized. The lipid metabolites in the homogenates were added into pre-washed solid phase extraction HLB cartridges (Waters® Oasis), washed, eluted, and dried using a centrifugal vacuum evaporator. The LC-MS/MS analysis was performed using an Agilent 1200SL HPLC system (Agilent) coupled with a 4000 QTRAP MS/MS (AB Sciex). The concentrations of the lipid metabolites were calculated using the standard calibration curve.

2.3 Total RNA isolation and quantitative PCR analysis

The proximal section of small intestine was dissected and grounded after being frozen by liquid nitrogen. The TRIzol reagent (Ambion, Austin, TX) was used to isolate the total RNA and the High-Capacity cDNA Reverse Transcription kit (Applied Biosystems) was used to reverse transcribe the isolated RNA into cDNA. qRT-PCR was performed in the CFX96™ Real-Time PCR Detection System (Bio-Rad Laboratories) and final gene expression results were calculated using the $2^{-\triangle Ct}$ method. The information on primers is listed in Table S1.

2.4 Tissue staining

The tissue fixation, paraffin embedding, section, dewaxing, and antigen retrieval were performed as described (Wang et al., 2018b). The immunohistochemistry staining was conducted using HRP/DAB (ABC) Detection IHC kit (Abcam) according to the manufacturer's instruction. The anti-Lysozyme antibody (Invitrogen, catalog # MA5-32154), anti-F4/80 antibody (Cell Signaling, catalog # 70076), or anti-sEH antibody (Santa Cruz Biotechnology, catalog # sc-166961) was used to probe the target protein in tissue section.

The number of Lysozyme^{+} cells was counted from crypts taken randomly from 4-5 mice per group. The staining intensity of F4/80 and sEH was analyzed by Image J software using IHC Toolbox.

2.5 Flow cytometry analysis

The intestinal immune cells were released and prepared as previous study (Wang et al., 2018b). The isolated cells were stained using anti-mouse CD45 antibody (FITC-conjugated, BioLegend, catalog # 103108) or control isotype antibody (BioLegend, catalog # 400605), and then analyzed with BD FACSCanto™ II cell analyzer (BD Biosciences). All the flow cytometry data were analyzed using FlowJo software (FlowJo LLC).

2.6 Statistical analysis

All data are reported as the mean ± standard error of the mean (SEM). The normality of data was determined by Shapiro-Wilk test and the equal variance of data was checked by Levene's mean test before the statistical analysis. Statistical comparison of two groups was assessed by either Student's *t* test or Wilcoxon-Mann-Whitney test (if the normality test failed). Statistical comparison of three groups was analyzed using one-way ANOVA followed by Tukey's or Fisher's post hoc test, or using Kruskal-Wallis test on Ranks (if the normality test failed) followed by appropriate post hoc test. All data analysis was conducted using SigmaPlot software (Systat Software, Inc).

3. Results

3.1 AFB$_1$ suppresses M2 macrophages in intestine

We orally exposed the C57BL/6 mice to multiple doses of AFB$_1$ via drinking water for 21 days (Fig. 1A). The concentration of AFB$_1$ in water was 0.5, 1.5, or 5 mg/L, which was calculated to deliver AFB$_1$ at estimated doses of 0.06, 0.18, or 0.6 mg/kg body weight (b.w.) per day, respectively. The AFB$_1$ exposure dose and time were selected based on previous intestinal barrier function studies using the concentration range of 0.5 to 2 mg/L in the diet in chicken models, and dose range of 0.2 to 0.5 mg/kg b.w. in rat or ICR mouse model with exposure time from 14 to 28 days (Table S2). Moreover, the doses were similar to the estimated cumulative exposure dose of AFB$_1$ in humans (0.13-0.49 mg/kg b.w.) (Ming et al., 2002), supporting that it is feasible to apply this treatment scheme to model human exposure to AFB$_1$.

We first investigated the effect of AFB$_1$ on intestinal immune function by determining the profile of intestinal resident immune cells. Flow cytometry analysis showed that AFB$_1$ dose-dependently reduced CD45^{+} total immune cells in the intestine (Fig. 1B–C). Further analysis of immune cell subsets showed that AFB$_1$ decreased the expression of *F4/80* (a macrophage marker) and *Cd3* (a T cell marker), while it had little effect on *Cd19* (a B cell marker) or *Ly6g* (a neutrophil marker) (Fig. 1D). Similar to the qRT-PCR result, immunohistochemical analysis showed that AFB$_1$ reduced abundance of F4/80[+] macrophages in the intestine (Fig. 1E–F). Macrophage polarization analysis showed that AFB$_1$ exposure reduced the M2 macrophages (*Cd163*, *Cd206*) and attenuated M2-associated cytokines (*Tgf-β*, *Arg1*), while it had little effect on the M1 macrophages (*Cd80*, *Cd86*) or associated cytokines (*Il-1β*,

Il-6, Tnf-α) (Fig. 1G–H). Together, these results demonstrate that AFB$_1$ exposure reduces macrophages, notably the M2 macrophages, in intestine.

3.2 AFB$_1$ decreases Paneth cells and antimicrobial peptides in intestine

Having demonstrated the detrimental effects of AFB$_1$ on macrophages, we studied its effects on Paneth cells, a specialized epithelial lineage in the base of the crypts, which maintain the homeostasis of intestinal host-microbial interface by sensing intestinal microorganisms and secreting antimicrobial peptides (39). Immunohistochemical staining showed that AFB$_1$ dose-dependently reduced the intestinal abundance of lysozyme$^+$ Paneth cells (Fig. 2A–B). Consistent with the immunohistochemical result, qRT-PCR showed that AFB$_1$ reduced gene expression of *lysozyme*, a marker of Paneth cells, in intestinal tissues (Fig. 2C). Furthermore, AFB$_1$ exposure decreased the expressions of *α-defensins-3, β-defensins-1, REG3β* and *REG3γ*, which encode Paneth cells-derived antimicrobial peptides, in the intestine (Fig. 2D). Together, these results support that AFB$_1$ exposure reduces both abundance and antimicrobial activity of Paneth cells in the intestine.

3.3 AFB$_1$ elevates sEH in intestine

As a membrane-active compound, AFB$_1$ is capable of releasing free arachidonic acid and activating eicosanoid metabolism pathways (Amstad et al., 1984; Iida et al., 1998; Liu et al., 1990). To explore the involvement of eicosanoids in AFB$_1$ immunotoxicity, we used an oxylipinomics approach to systematically determine the eicosanoid profile in the intestine tissues of vehicle- and AFB$_1$-exposed (5 mg/L) mice. We quantified 75 eicosanoids in intestinal tissues (Table S3, some eicosanoids were below the detection limit). Oxylipin analysis showed that exposure to AFB$_1$ decreased the levels of EpFAs, including epoxyeicosatrienoic acids (EETs) derived from ARA, epoxyeicosatetraenoic acids (EEQs) derived from EPA, epoxydocosapentaenoic acids (EDPs) derived from DHA, epoxyoctadecadienoic acids (EpODEs) from ALA, and epoxyoctadecamonoenoic acids (EpOMEs) derived from LA, in intestine (Fig. 3A–F, Table S3). Besides EpFAs, AFB$_1$ exposure also modulated the levels of certain LOX-derived lipid metabolites while it had little effect on COX-derived metabolites in intestine (Table S3).

To understand the mechanisms by which AFB$_1$ reduced intestinal levels of EpFAs, we determined the expression of enzymes controlling the biosynthesis and degradation of EpFAs (Fig. 3A). EpFAs are produced by CYP monooxygenases (largely but not exclusively CYP2C and CYP2J isoforms) and are largely hydrolyzed by sEH. qRT-PCR showed that AFB$_1$ increased *Ephx2* (encoding sEH) expression (Fig. 3G), while it had little effect on *Cyp2c* and *Cyp2j* expression, in intestinal tissues (Fig. S2). Immunohistochemical analysis further showed that AFB$_1$ increased the protein level of sEH in the intestine (Fig. 3H). We also measured the expression of microsomal epoxide hydrolase (mEH, encoded by the *Ephx1* gene*)*, which plays a key role in AFB$_1$ detoxification (Kelly et al., 2002). We found that AFB$_1$ exposure had little effect on the expression of *Ephx1* in intestine (Fig. S3). Together, these results demonstrate that AFB$_1$ exposure elevates intestinal expression of sEH, resulting in reduced levels of EpFAs in the intestine.

3.4   Genetic knockout of sEH attenuates the toxic effects of AFB$_1$ on intestinal immunity

Having demonstrated that AFB$_1$ elevated sEH in intestines, we studied the function of sEH in AFB$_1$-induced mucosal immunotoxicity. We treated wild-type (WT) or *Ephx2* $^{-/-}$ mice with AFB$_1$ (5 mg/L) for 21 days (Fig. 4A). In WT mice, AFB$_1$ exposure diminished intestinal resident macrophages, especially the cell markers of M2 macrophages, and suppressed the expression of *Tgf-β* (Fig. 4B–E), while AFB$_1$ had little effect on the cell markers of M1 macrophages and B cells (Fig. S4). Moreover, AFB$_1$ reduced the abundance of lysozyme$^+$ Paneth cells, decreased the expression of the antimicrobial peptides *α-defensin-3* and *β-defensin-1* (Fig. 4F–H). However, all these effects were attenuated by sEH deficiency (Fig. 4B–H). Overall, these results support that sEH is required for AFB$_1$'s toxic effect on intestinal immunity.

3.5   Pharmacological inhibition of sEH alleviates AFB$_1$-induced intestinal immunotoxicity

To achieve translation to humans and farm animals, we examined the efficacy of pharmacological inhibition of sEH using a highly potent and selective small-molecule inhibitor TPPU (Fig. 5A). We found that co-administration of TPPU inhibited the toxic effects of AFB$_1$ on intestinal M2 microphage by rescuing the AFB$_1$-attenuated expressions of *F4/80*, *Cd163* and *Cd206* (Fig. 5B–C), while it had little effect on the M1 macrophage markers (*Cd80, Cd86*) and the B cell marker (*Cd19*) (Fig. S5). Moreover, TPPU increased the AFB$_1$-suppressed lysozyme$^+$ Paneth cell abundance and *α-defensin-3* expression in intestine (Fig. 5D–F), while has limited effect on the *Tgf-β* and *β-defensin-3* (Fig. S6). Together, these results support that sEH pharmacological inhibitor has protective effects against AFB$_1$ immunotoxicity in intestine.

4.   Discussion

Contamination of food products with AFB$_1$ is common in many areas of the world. This results in serious health issues as well as major losses of food products when they are rejected because of AFB$_1$ contamination. The intestinal mucosa serves as the predominant host immune defense system, while it is also a vulnerable tissue challenged by oral exposure to AFB$_1$ in contaminated food. However, the detailed toxic mechanism and endogenous regulators are still elusive. Here our central finding is that AFB$_1$ exposure suppressed intestinal immune function by impairing M2 macrophages and Paneth cells, which parallels the activation of sEH-mediated epoxy fatty acid metabolism. Moreover, sEH deficiency or inhibition blocks the AFB$_1$ toxicity by preserving M2 macrophages and Paneth cells in intestine. Together, these data demonstrate that sEH contributes to AFB$_1$-induced intestinal immunity defects.

Intestinal resident macrophages play a crucial role in mucosal defenses against intestinal infection. Here, we found that AFB$_1$ decreased the population of intestinal macrophages, especially the M2 macrophage and the resulting cytokines. Given that M2 macrophages are featured by potent phagocytosis and pathogen clearing capacity (Roszer, 2015), our finding agrees with previous studies showing that AFB$_1$ exposure suppressed the uptake of *Staphylococcus aureus* and microbicidal activity of macrophages *in vitro* (Cusumano et al., 1996; Pang et al., 2020), and compromised the phagocytosis activity of macrophages

in vivo (Jakab et al., 1994; Neldon-Ortiz and Qureshi, 1992; Richard and Thurston, 1975; Ul-Hassan et al., 2012). Importantly, we found that sEH deficiency or inhibition restored the population of M2 macrophages. Similar to our finding, previous studies showed that sEH inhibition promoted M2 macrophage polarization both *in vitro* (Wang et al., 2018a) and *in vivo* (Lopez-Vicario et al., 2015; Yeh et al., 2019). Parallel with M2 polarization, treatment of TPPU enhanced macrophage phagocytic ability in a cecal puncture-induced sepsis model (Chen et al., 2020). Remarkably, our recent studies identified that dual inhibition of sEH and COX-2 enhanced macrophage phagocytosis of AFB_1-induced hepatocyte debris (Fishbein et al., 2020). Together, our findings, along with the previous research, support that blocking the sEH activity could be an effective strategy for improving the intestinal pathogen clearing capacity by enhancing AFB_1-suppressed M2 macrophages.

In addition to macrophages, the Paneth cell is responsible for producing a series of antimicrobial peptides to eliminate pathogenic microorganisms from penetrating both mucus and epithelial layers (Bevins and Salzman, 2011). Here, we found AFB_1 exposure decreased lysozyme$^+$ cells at the base of intestinal crypts, indicating dysfunction of Paneth cells. Our finding is consistent with the electron microscopic evidence showing the irregular hyperchromatic nuclei and damaged secretory granules of Paneth cells in AFB_1-exposed rats (Yassien et al., 2020). In line with the impaired Paneth cells, we observed decreased antimicrobial peptide expression, notably *α-defensins-3* and *β-defensins-1*, in AFB_1-exposed mice. Both α- and β-defensins have antimicrobial activities toward bacteria, fungi, and enveloped viruses (Lehrer and Ganz, 1996). Moreover, a recent study showed that defensin-like anti-microbial peptide CopA3 attenuated the AFB_1-induced colon toxicity in mice (Dey et al., 2021). Thus, disrupted Paneth cells and suppressed antimicrobial peptide expression due to AFB_1 exposure could lead to increased risks of pathogen invasion and infection. Indeed, human and animal studies showed that dietary AFB_1 exposure impaired host defense and caused increased susceptibility to intestinal pathogen infections (Accardi et al., 2015; Boonchuvit and Hamilton, 1975; Cysewski et al., 1978; Rao et al., 1995; Ruff, 1978). Promisingly, sEH deficiency or inhibition restored the Paneth cells and expression of antimicrobial peptides, especially *α-defensins-3*, which could help to protect against pathogen infections. This finding agrees with previous studies showing that treatment of TPPU diminished bacterial dissemination, alleviated organ damage, and improved the survival rate of mice in a cecal puncture-induced sepsis model (Chen et al., 2020). Additionally, pharmacological inhibition of sEH reduced periodontitis induced by *Aggregatibacter actinomycetemcomitans* in a mouse model (Trindade-da-Silva et al., 2017). A limitation of the current study is that we mainly detected the expression of cytokines and antimicrobial peptides using mRNA levels. Further studies are needed to better characterize these immunological modulators in protein levels and determine the detailed molecular basis by which sEH regulates M2 macrophage cytokines or Paneth cell-produced antimicrobial peptides. Together, we identified that deficiency or inhibition of sEH restored the AFB_1-disrupted Paneth cell function and antimicrobial peptide production, which could help to strengthen the host defenses against intestinal pathogen invasion and infections.

Here, we showed that sEH plays a critical role in mediating AFB_1 immunotoxicity in intestine. In agreement with our findings, previous studies showed that sEH is actively involved in the pathology of various intestinal diseases and pathologies. sEH has been

shown to be up-regulated under intestinal inflammation, ulceration, and allergic reaction in both patients and pre-clinical models (Bastan et al., 2018; Wang et al., 2018b; Zhang et al., 2013a). Moreover, sEH deficiency or inhibition reduced the inflammation and ulcer formation in nonsteroidal anti-inflammatory drugs-, dextran sulfate sodium-, *Il10* knockout-, obesity- or food allergen-induced intestinal illness (Bastan et al., 2018; Goswami et al., 2016; Reisdorf et al., 2019; Wang et al., 2020; Zhang et al., 2013a; Zhang et al., 2013b; Zhang et al., 2012). These studies support the hypothesis that the sEH enzyme acts as both a marker and a cause of dysfunction in various intestinal diseases. Acting as an eicosanoid metabolizing enzyme, sEH is responsible for converting EpFAs into less bioactive dihydroxy fatty acids (Morisseau and Hammock, 2013). Akin to the increased intestinal expression of sEH, oxylipin profiling revealed decreased levels of EpFAs, including EETs, EEQs, EDPs, EpODEs and EpOMEs, in intestinal tissues from AFB_1-exposed mice. Accumulating evidence support that EpFAs, especially the EETs and EEQs, play vital roles in regulating immune function. Indeed, treatment of EETs promote macrophage phenotype from M1 to M2 polarization, regulate the phagocytosis and facilitate uptake of *E. coli* and *L. monocytogenes* in macrophages (Bystrom et al., 2013; Dai et al., 2015). Moreover, administration of 17,18-EEQ decreased the severity of ovalbumin-induced intestinal allergic diarrhea in mice (Kunisawa et al., 2015). Thus, decreased levels and attenuated protective effects of EpFAs could be a major mechanism contributing to AFB_1 immunotoxicity in intestine. In addition to EpFAs, a previous study showed that dihydroxyeicosatrienoic acid (DHETs), the sEH-derived lipid metabolites, caused gut barrier permeability and bacterial translocation in mice (Wang et al., 2020). Further studies are needed to determine the detailed effect of EpFAs and DHETs on intestinal immune function following AFB_1 exposure. Moreover, future studies using the quantitative food-based AFB_1 exposure approach are warranted to mimic the real human exposure condition and to determine the effect of sEH inhibition on AFB_1 food contamination-caused intestinal disorders.

5. Conclusion

In summary, our study demonstrates that AFB_1 disrupts intestinal immune function by suppressing the M2 and Paneth cells. Moreover, we show that AFB_1 causes intestinal immunotoxicity, in part, by leading to a dramatic increase in sEH protein and decrease in inflammation-resolving EpFAs. This is of practical importance given that sEH inhibitors are in clinical development for targeting a series of diseases in humans and domestic animals (Chen et al., 2012; Guedes et al., 2013; Hammock et al., 2021; Lazaar et al., 2016; McReynolds et al., 2019). Moreover, recent publications demonstrated that natural sEH inhibitors, extracted from *Lepidium meyenii (maca)* or roots of *Pentadiplandra brazzeana*, effectively reduced LPS-induced inflammatory disease in rodent models (Kitamura et al., 2017; Kitamura et al., 2015; Singh et al., 2020). There are also several new classes of natural sEH inhibitors, notably kurarinone, effective in attenuating neuroinflammation (Sun et al., 2022). These findings indicate an attractive direction to further investigate and develop natural sEH inhibitor-based food additives as an economical approach to protect farm animals and humans from AFB_1 toxicity. Altogether, our study supports pharmacological targeting of sEH as a promising strategy in alleviating AFB_1 intestinal immunotoxicity.

Supplementary Material

Refer to Web version on PubMed Central for supplementary material.

Acknowledgments

References

Accardi R, et al. , 2015. The mycotoxin aflatoxin B1 stimulates Epstein-Barr virus-induced B-cell transformation in in vitro and in vivo experimental models. Carcinogenesis. 36, 1440–51. [PubMed: 26424750]

Amstad P, et al. , 1984. Evidence for membrane-mediated chromosomal damage by aflatoxin B1 in human lymphocytes. Carcinogenesis. 5, 719–23. [PubMed: 6426812]

Bastan I, et al. , 2018. Inhibition of soluble epoxide hydrolase attenuates eosinophil recruitment and food allergen-induced gastrointestinal inflammation. J Leukoc Biol. 104, 109–122. [PubMed: 29345370]

Bevins CL, Salzman NH, 2011. Paneth cells, antimicrobial peptides and maintenance of intestinal homeostasis. Nat Rev Microbiol. 9, 356–68. [PubMed: 21423246]

Boonchuvit B, Hamilton PB, 1975. Interaction of aflatoxin and paratyphoid infections in broiler chickens. Poult Sci. 54, 1567–73. [PubMed: 810786]

Bystrom J, et al. , 2013. Inducible CYP2J2 and its product 11,12-EET promotes bacterial phagocytosis: a role for CYP2J2 deficiency in the pathogenesis of Crohn's disease? PLoS One. 8, e75107. [PubMed: 24058654]

Chen D, et al. , 2012. Pharmacokinetics and pharmacodynamics of AR9281, an inhibitor of soluble epoxide hydrolase, in single- and multiple-dose studies in healthy human subjects. J Clin Pharmacol. 52, 319–28. [PubMed: 21422238]

Chen Z, et al. , 2020. sEH Inhibitor Tppu Ameliorates Cecal Ligation and Puncture-Induced Sepsis by Regulating Macrophage Functions. Shock. 53, 761–771. [PubMed: 31318834]

Cusumano V, et al. , 1996. Immunobiological activities of mould products: functional impairment of human monocytes exposed to aflatoxin B1. Res Microbiol. 147, 385–91. [PubMed: 8763624]

Cysewski SJ, et al. , 1978. Effects of aflatoxin on the development of acquired immunity to swine erysipelas. Am J Vet Res. 39, 445–8. [PubMed: 637393]

Dai M, et al. , 2015. Epoxyeicosatrienoic acids regulate macrophage polarization and prevent LPS-induced cardiac dysfunction. J Cell Physiol. 230, 2108–19. [PubMed: 25626689]

Dennis EA, Norris PC, 2015. Eicosanoid storm in infection and inflammation. Nat Rev Immunol. 15, 511–23. [PubMed: 26139350]

Dey DK, et al. , 2021. The inflammation response and risk associated with aflatoxin B1 contamination was minimized by insect peptide CopA3 treatment and act towards the beneficial health outcomes. Environ Pollut. 268, 115713. [PubMed: 33038573]

Fishbein A, et al. , 2020. Resolution of eicosanoid/cytokine storm prevents carcinogen and inflammation-initiated hepatocellular cancer progression. Proc Natl Acad Sci U S A. 117, 21576–21587. [PubMed: 32801214]

Goswami SK, et al. , 2016. Anti-Ulcer Efficacy of Soluble Epoxide Hydrolase Inhibitor TPPU on Diclofenac-Induced Intestinal Ulcers. J Pharmacol Exp Ther. 357, 529–36. [PubMed: 26989141]

Guedes AG, et al. , 2013. Use of a soluble epoxide hydrolase inhibitor as an adjunctive analgesic in a horse with laminitis. Vet Anaesth Analg. 40, 440–8. [PubMed: 23463912]

Hammock BD, et al. , 2021. Movement to the Clinic of Soluble Epoxide Hydrolase Inhibitor EC5026 as an Analgesic for Neuropathic Pain and for Use as a Nonaddictive Opioid Alternative. J Med Chem. 64, 1856–1872. [PubMed: 33550801]

Harizi H, et al. , 2008. Arachidonic-acid-derived eicosanoids: roles in biology and immunopathology. Trends Mol Med. 14, 461–9. [PubMed: 18774339]

Iida N, et al. , 1998. Suppression of arachidonic acid cascade-mediated apoptosis in aflatoxin B1-induced rat hepatoma cells by glucocorticoids. Carcinogenesis. 19, 1191–202. [PubMed: 9683177]

Jakab GJ, et al. , 1994. Respiratory aflatoxicosis: suppression of pulmonary and systemic host defenses in rats and mice. Toxicol Appl Pharmacol. 125, 198–205. [PubMed: 8171428]

Jiang M, et al. , 2015a. Effect of aflatoxin B(1) on IgA(+) cell number and immunoglobulin mRNA expression in the intestine of broilers. Immunopharmacol Immunotoxicol. 37, 450–7. [PubMed: 26357012]

Jiang M, et al. , 2015b. Effects of aflatoxin b1 on T-cell subsets and mRNA expression of cytokines in the intestine of broilers. Int J Mol Sci. 16, 6945–59. [PubMed: 25826527]

Jiang XS, et al. , 2020. Inhibition of soluble epoxide hydrolase attenuates renal tubular mitochondrial dysfunction and ER stress by restoring autophagic flux in diabetic nephropathy. Cell Death Dis. 11, 385. [PubMed: 32439839]

Kelly EJ, et al. , 2002. Expression of human microsomal epoxide hydrolase in Saccharomyces cerevisiae reveals a functional role in aflatoxin B1 detoxification. Toxicol Sci. 65, 35–42. [PubMed: 11752683]

Kitamura S, et al. , 2017. Occurrence of urea-based soluble epoxide hydrolase inhibitors from the plants in the order Brassicales. PLoS One. 12, e0176571. [PubMed: 28472063]

Kitamura S, et al. , 2015. Potent natural soluble epoxide hydrolase inhibitors from Pentadiplandra brazzeana baillon: synthesis, quantification, and measurement of biological activities in vitro and in vivo. PLoS One. 10, e0117438. [PubMed: 25659109]

Kumagai S, 1989. Intestinal absorption and excretion of aflatoxin in rats. Toxicol Appl Pharmacol. 97, 88–97. [PubMed: 2492684]

Kunisawa J, et al. , 2015. Dietary omega3 fatty acid exerts anti-allergic effect through the conversion to 17,18-epoxyeicosatetraenoic acid in the gut. Sci Rep. 5, 9750. [PubMed: 26065911]

Lazaar AL, et al. , 2016. Pharmacokinetics, pharmacodynamics and adverse event profile of GSK2256294, a novel soluble epoxide hydrolase inhibitor. Br J Clin Pharmacol. 81, 971–9. [PubMed: 26620151]

Lee KS, et al. , 2014. Optimized inhibitors of soluble epoxide hydrolase improve in vitro target residence time and in vivo efficacy. J Med Chem. 57, 7016–30. [PubMed: 25079952]

Lehrer RI, Ganz T, 1996. Endogenous vertebrate antibiotics. Defensins, protegrins, and other cysteine-rich antimicrobial peptides. Ann N Y Acad Sci. 797, 228–39. [PubMed: 8993365]

Liu L, et al. , 1990. In vitro prostaglandin H synthase- and monooxygenase-mediated binding of aflatoxin B1 to DNA in guinea-pig tissue microsomes. Carcinogenesis. 11, 1915–9. [PubMed: 2121380]

Lopez-Vicario C, et al. , 2015. Inhibition of soluble epoxide hydrolase modulates inflammation and autophagy in obese adipose tissue and liver: role for omega-3 epoxides. Proc Natl Acad Sci U S A. 112, 536–41. [PubMed: 25550510]

McReynolds CB, et al. , 2019. Pharmaceutical Effects of Inhibiting the Soluble Epoxide Hydrolase in Canine Osteoarthritis. Front Pharmacol. 10, 533. [PubMed: 31214021]

Ming L, et al. , 2002. Dominant role of hepatitis B virus and cofactor role of aflatoxin in hepatocarcinogenesis in Qidong, China. Hepatology. 36, 1214–20. [PubMed: 12395332]

Morisseau C, Hammock BD, 2013. Impact of soluble epoxide hydrolase and epoxyeicosanoids on human health. Annu Rev Pharmacol Toxicol. 53, 37–58. [PubMed: 23020295]

Mwanda OW, et al. , 2005. Acute aflatoxicosis: case report. East Afr Med J. 82, 320–4. [PubMed: 16175785]

Neldon-Ortiz DL, Qureshi MA, 1992. Effects of AFB1 embryonic exposure on chicken mononuclear phagocytic cell functions. Dev Comp Immunol. 16, 187–96. [PubMed: 1499838]

Pang VF, et al. , 2020. The in vitro effects of aflatoxin B1 on physiological functions of swine alveolar macrophages. Vet Med Sci. 6, 919–925. [PubMed: 32594663]

Rao JR, et al. , 1995. Influence of dietary aflatoxin on Eimeria uzura infection in Japanese quail (Coturnix coturnix japonica). Vet Parasitol. 56, 17–22. [PubMed: 7732641]

Reisdorf WC, et al. , 2019. Preclinical evaluation of EPHX2 inhibition as a novel treatment for inflammatory bowel disease. PLoS One. 14, e0215033. [PubMed: 31002701]

Richard JL, Thurston JR, 1975. Effect of aflatoxin on phagocytosis of Aspergillus fumigatus spores by rabbit alveolar macrophages. Appl Microbiol. 30, 44–7. [PubMed: 1096823]

Rose TE, et al. , 2010. 1-Aryl-3-(1-acylpiperidin-4-yl)urea inhibitors of human and murine soluble epoxide hydrolase: structure-activity relationships, pharmacokinetics, and reduction of inflammatory pain. J Med Chem. 53, 7067–75. [PubMed: 20812725]

Roszer T, 2015. Understanding the Mysterious M2 Macrophage through Activation Markers and Effector Mechanisms. Mediators Inflamm. 2015, 816460. [PubMed: 26089604]

Ruff MD, 1978. Influence of dietary aflatoxin on the severity of Eimeria acervulina infection in broiler chickens. Avian Dis. 22, 471–80. [PubMed: 697658]

Sheppe AEF, Edelmann MJ, 2021. Roles of Eicosanoids in Regulating Inflammation and Neutrophil Migration as an Innate Host Response to Bacterial Infections. Infect Immun. 89, e0009521. [PubMed: 34031130]

Singh N, et al. , 2020. N-Benzyl-linoleamide, a Constituent of Lepidium meyenii (Maca), Is an Orally Bioavailable Soluble Epoxide Hydrolase Inhibitor That Alleviates Inflammatory Pain. J Nat Prod. 83, 3689–3697. [PubMed: 33320645]

Sun CP, et al. , 2022. Kurarinone alleviated Parkinson's disease via stabilization of epoxyeicosatrienoic acids in animal model. Proc Natl Acad Sci U S A. 119.

Tomkova I, et al. , 2002. Effect of aflatoxin B1 on CD3 T cells and alkaline phosphatase in the intestine of mice. Mycopathologia. 154, 15–9. [PubMed: 12041866]

Trindade-da-Silva CA, et al. , 2017. Soluble Epoxide Hydrolase Pharmacological Inhibition Decreases Alveolar Bone Loss by Modulating Host Inflammatory Response, RANK-Related Signaling, Endoplasmic Reticulum Stress, and Apoptosis. J Pharmacol Exp Ther. 361, 408–416. [PubMed: 28356494]

Ul-Hassan Z, et al. , 2012. Immunological status of the progeny of breeder hens kept on ochratoxin A (OTA)- and aflatoxin B(1) (AFB(1))-contaminated feeds. J Immunotoxicol. 9, 381–91. [PubMed: 22530919]

Wang L, et al. , 2012. Use of a soluble epoxide hydrolase inhibitor in smoke-induced chronic obstructive pulmonary disease. Am J Respir Cell Mol Biol. 46, 614–22. [PubMed: 22180869]

Wang Q, et al. , 2018a. Expression of soluble epoxide hydrolase in renal tubular epithelial cells regulates macrophage infiltration and polarization in IgA nephropathy. Am J Physiol Renal Physiol. 315, F915–F926. [PubMed: 29717935]

Wang W, et al. , 2018b. Lipidomic profiling reveals soluble epoxide hydrolase as a therapeutic target of obesity-induced colonic inflammation. Proc Natl Acad Sci U S A. 115, 5283–5288. [PubMed: 29717038]

Wang Y, et al. , 2020. Soluble epoxide hydrolase is an endogenous regulator of obesity-induced intestinal barrier dysfunction and bacterial translocation. Proc Natl Acad Sci U S A. 117, 8431–8436. [PubMed: 32220957]

Wei J, Gronert K, 2019. Eicosanoid and Specialized Proresolving Mediator Regulation of Lymphoid Cells. Trends Biochem Sci. 44, 214–225. [PubMed: 30477730]

Williams JH, et al. , 2004. Human aflatoxicosis in developing countries: a review of toxicology, exposure, potential health consequences, and interventions. Am J Clin Nutr. 80, 1106–22. [PubMed: 15531656]

Yassien R, et al. , 2020. Histological and immunohistochemical study on the effect of Aflatoxin B1 on the ileum of adult male albino rat and possible protective effect of sodium selenite. Journal of Medical Histology. 4, 46–65.

Yeh CF, et al. , 2019. Soluble epoxide hydrolase inhibition enhances anti-inflammatory and antioxidative processes, modulates microglia polarization, and promotes recovery after ischemic stroke. Neuropsychiatr Dis Treat. 15, 2927–2941. [PubMed: 31686827]

Zhang W, et al. , 2013a. Soluble epoxide hydrolase deficiency inhibits dextran sulfate sodium-induced colitis and carcinogenesis in mice. Anticancer Res. 33, 5261–5271. [PubMed: 24324059]

Zhang W, et al. , 2013b. Reduction of inflammatory bowel disease-induced tumor development in IL-10 knockout mice with soluble epoxide hydrolase gene deficiency. Mol Carcinog. 52, 726–38. [PubMed: 22517541]

Zhang W, et al. , 2012. Soluble epoxide hydrolase gene deficiency or inhibition attenuates chronic active inflammatory bowel disease in IL-10(−/−) mice. Dig Dis Sci. 57, 2580–91. [PubMed: 22588244]
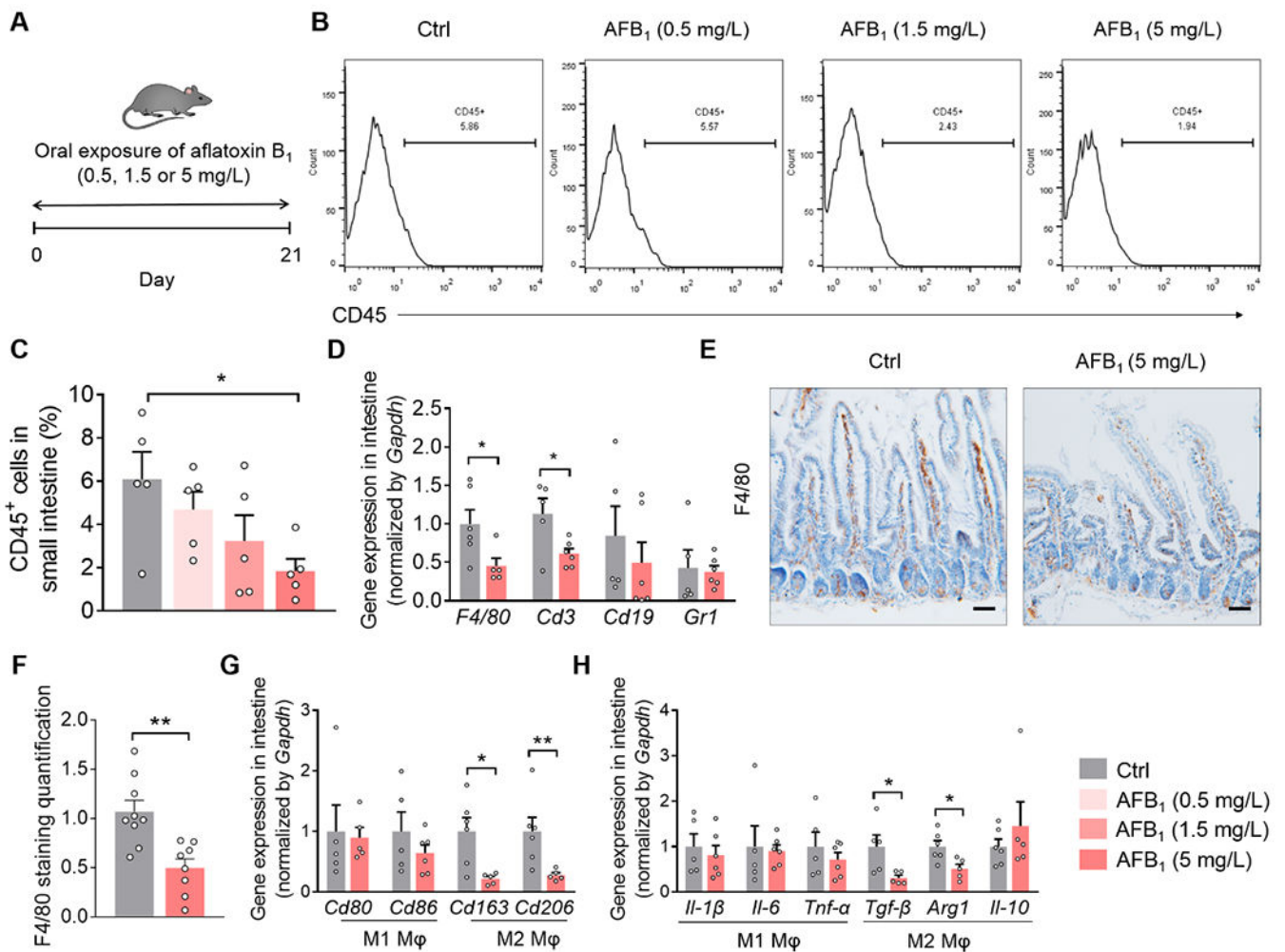
Figure 1. AFB$_1$ suppresses M2 macrophages in intestine.
(A) Scheme of animal experiment. C57BL/6 mice were orally treated with vehicle or AFB$_1$ (0.5, 1.5 or 5 mg/L) for 21 days. **(B)** Representative images of FACS analysis of CD45$^+$ cells in intestine. **(C)** FACS quantification of CD45$^+$ cell in intestine. **(D)** Gene expression of macrophage marker *F4/80*, T cell marker *Cd3*, B cell marker *Cd19*, and neutrophil marker *Ly6g* in intestine. **(E)** Representative microscopic images of immunohistochemical staining of F4/80$^+$ macrophages (magnification 200×, scale bars: 50 μm) in intestine. **(F)** quantification of F4/80 immunohistochemical staining intensity in intestine (n = 8-9 random fields per group). **(G)** Gene expression of M1 macrophage marker *Cd80, Cd86* and M2 macrophage marker *Cd163, Cd206* in intestine. **(H)** Gene expression of M1 macrophage-derived cytokines *Il-1β, Il-6, Tnf-α* and M2 macrophage-derived cytokines *Tgf-β, Arg1, Il-10* in intestine. The results are reported as mean ± SEM. n = 4-6 mice per group. * *P* < 0.05, ** *P* < 0.01.
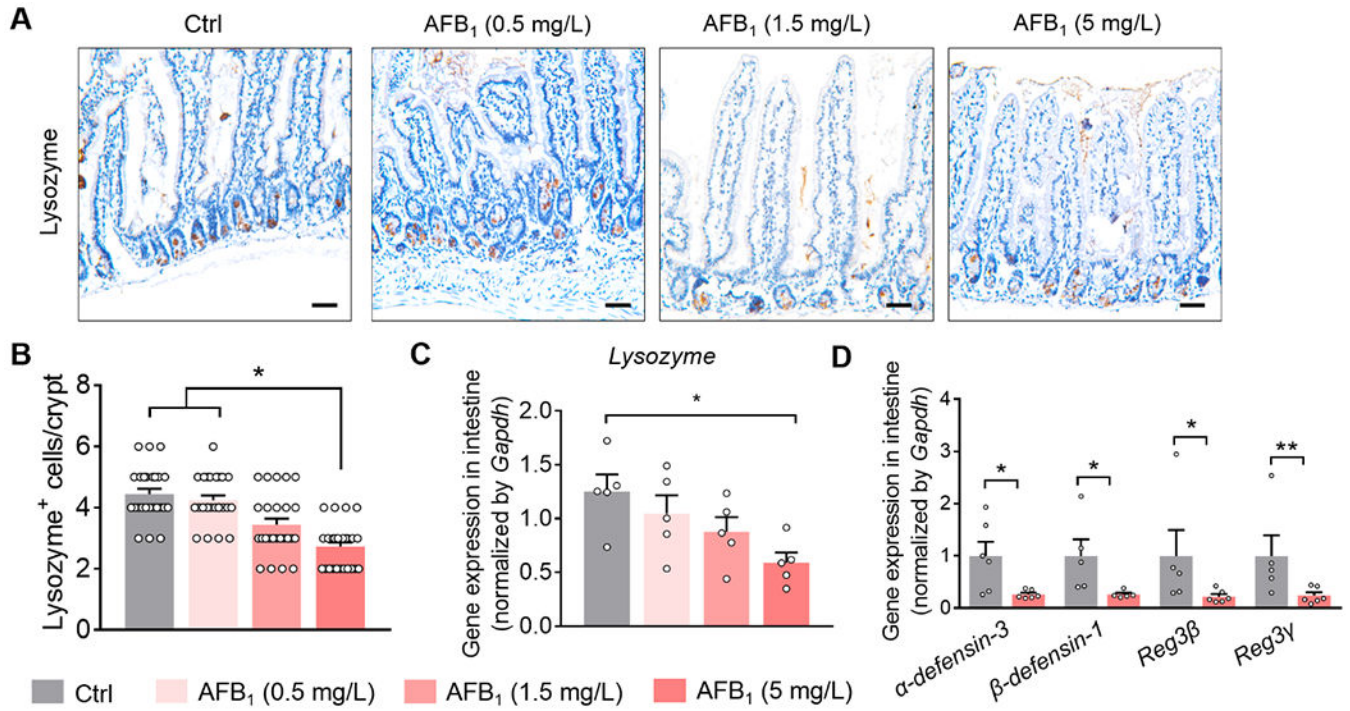
Figure 2. AFB$_1$ decreases Paneth cells and antimicrobial peptides in intestine.
(**A**) Representative microscopic images of immunohistochemical staining of lysozyme$^+$ Paneth cells (magnification 200×, scale bars: 50 μm) in intestine. (**B**) quantification of lysozyme$^+$ cells per crypt (n = 25 crypts per group). (**C**) Gene expression of Paneth cell marker *lysozyme* in intestine. (**D**) Gene expression of antimicrobial peptides *α-defensins-3, β-defensins-1, REG3β* and *REG3γ* in intestine. The results are reported as mean ± SEM. n = 4-6 mice per group. * *P* < 0.05, ** *P* < 0.01.
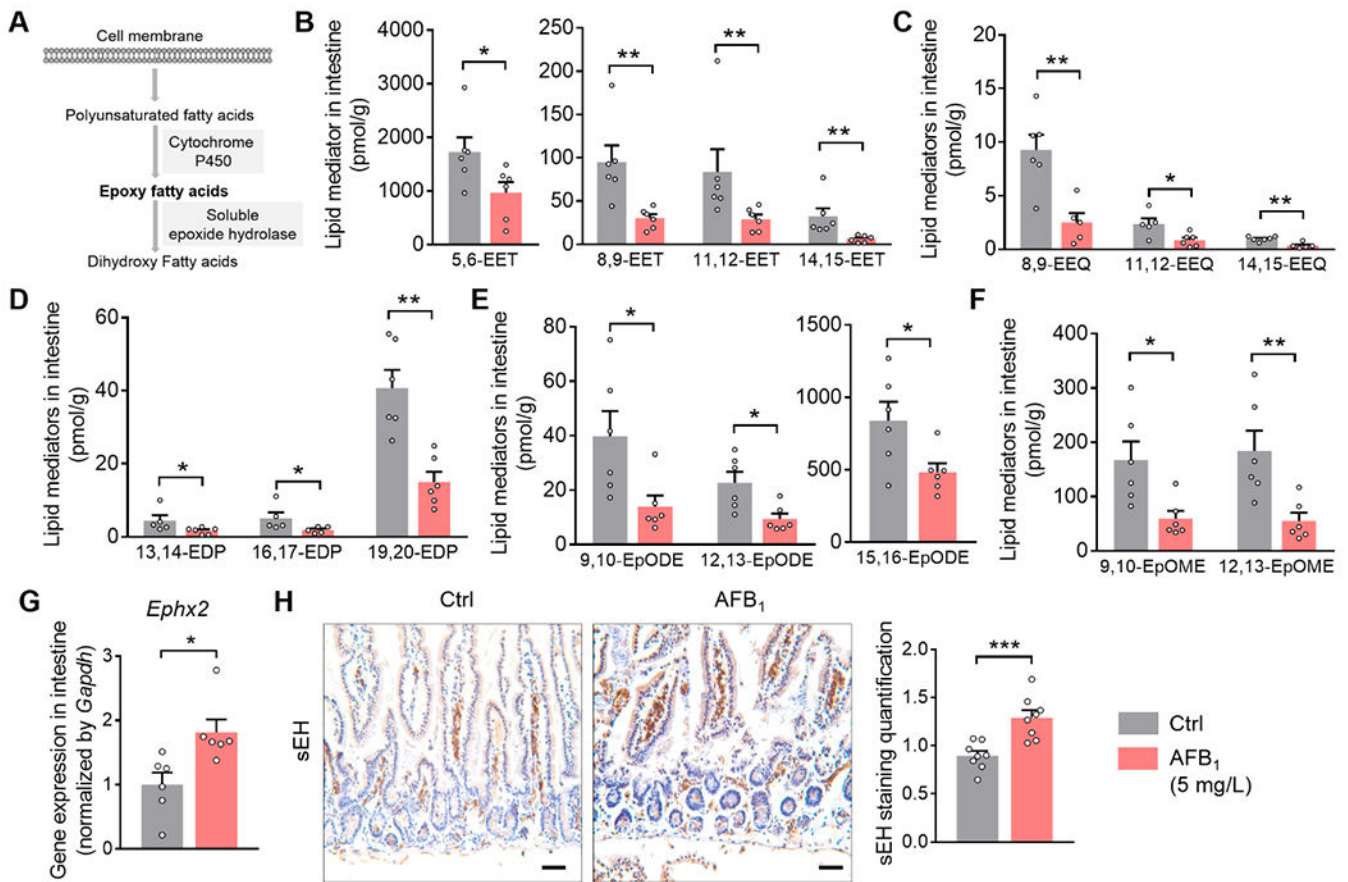
Figure 3. AFB$_1$ decreases EpFAs and elevates sEH in intestine.
(**A**) Scheme of epoxy fatty acids (EpFAs) biosynthesis and metabolism pathway.
(**B-F**) Quantification of (**B**) epoxyeicosatrienoic acid (EET) regioisomers, (**C**)
epoxyeicosatetraenoic acid (EEQ) regioisomers, (**D**) epoxydocosapentaenoic acid
(EDP) regioisomers, (**E**) epoxyoctadecadienoic acid (EpODE) regioisomers, (**F**)
epoxyoctadecamonoenoic acid (EpOME) regioisomers in intestine. (**G**) Gene expression of
Ephx2 in intestine. (**H**) Immunohistochemical staining of soluble epoxide hydrolase (sEH)
in intestine (magnification 200×, scale bars: 50 μm) and quantification of sEH staining
intensity in intestine (n = 8 random fields per group). The results are reported as mean ±
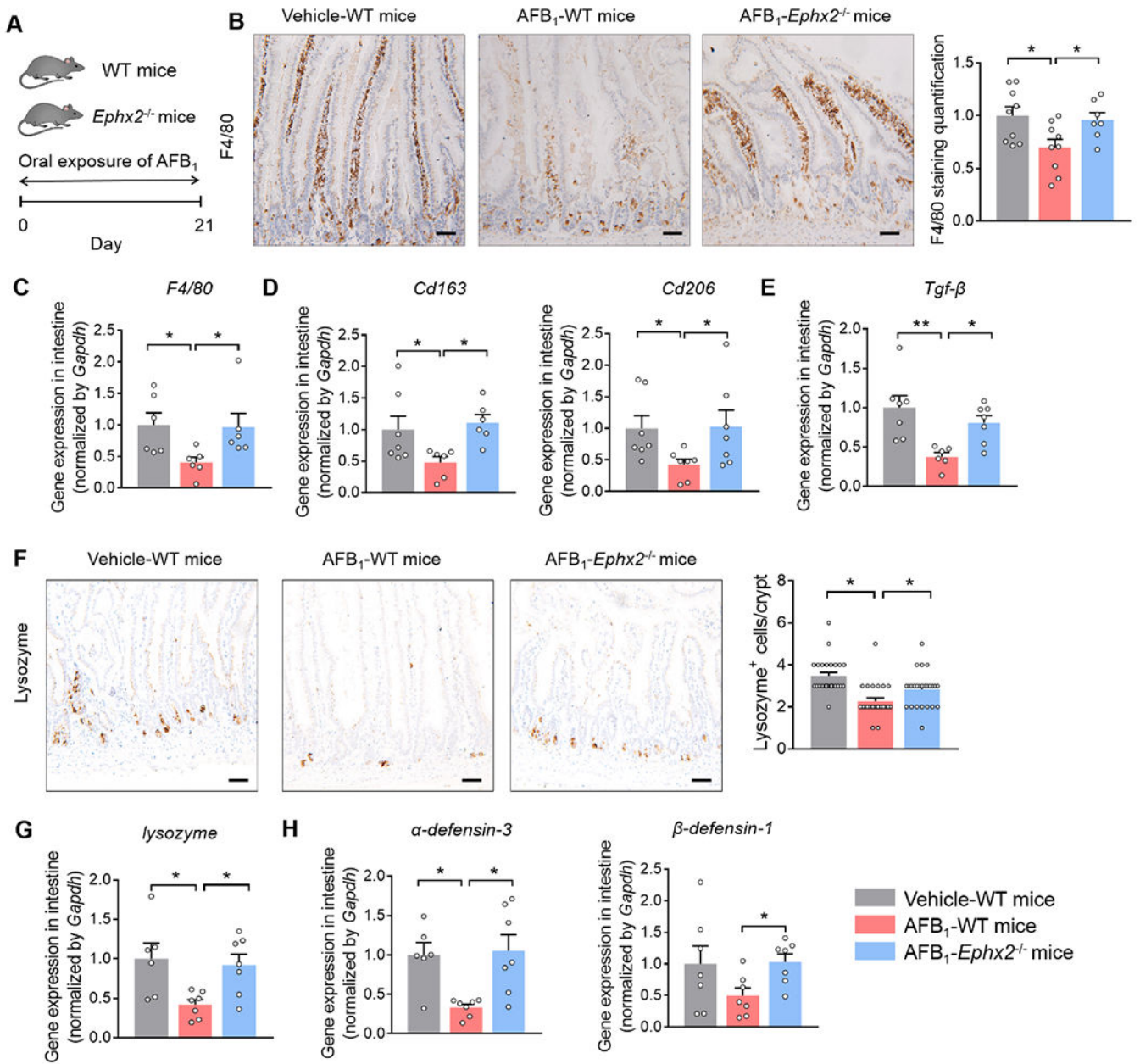SEM. n = 4-6 mice per group. * $P < 0.05$, ** $P < 0.01$, *** $P < 0.001$.

Figure 4. sEH deficiency abolishes the effects of AFB$_1$ on intestinal mucosal immunity.
(**A**) The scheme of animal experiment. Wild-type (WT) or *Ephx2*$^{-/-}$ C57BL/6 mice were orally treated with vehicle or AFB$_1$ (5 mg/L) for 21 days. (**B**) Immunohistochemical staining of F4/80 (magnification 200×, scale bars: 50 μm) and quantification of F4/80 staining intensity in intestine (n = 7-9 random fields per group). (**C**) Gene expression of macrophage marker *F4/80* in intestine. (**D**) Gene expression of M2 macrophage marker *Cd163* and *Cd206* in intestine. (**E**) Gene expression of *Tgf-β* in intestine. (**F**) Immunohistochemical staining of lysozyme in intestine (magnification 200×, scale bars: 50 μm) and quantification of lysozyme$^+$ cells per crypt (n = 25 units per group). (**G**) Gene expression of Paneth cell marker *lysozyme* in intestine. (**H**) Gene expression of antimicrobial peptides *α-defensins-3*

and *β-defensins-1* in intestine. The results are reported as mean ± SEM. n = 6-7 mice per group on gene expression analysis. * *P*< 0.05, ** *P*< 0.01.
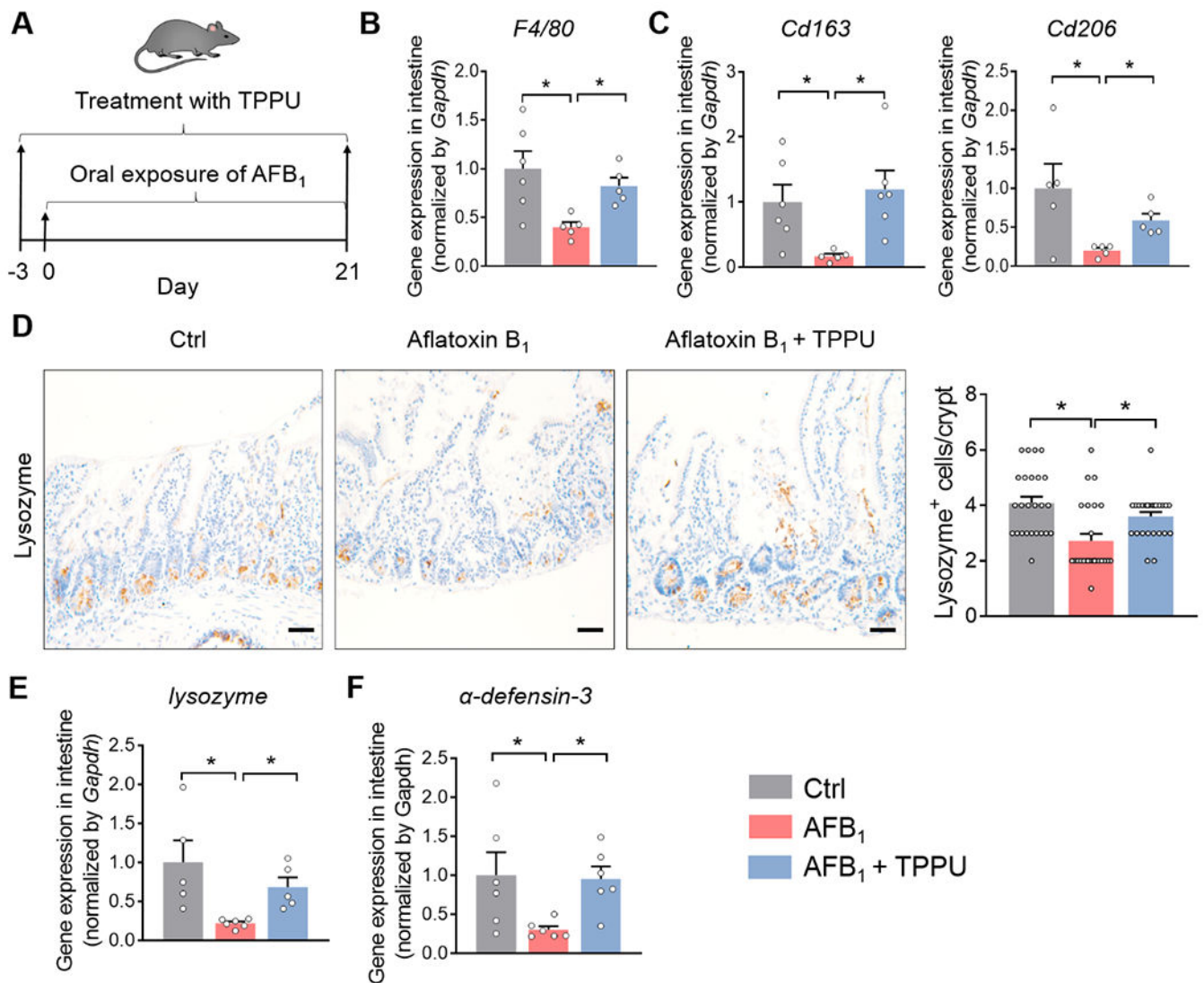
Figure 5. Pharmacological inhibition of sEH attenuates AFB1-suppressed intestinal immunity.
(**A**) Scheme of animal experiment. AFB_1 (5 mg/L)-exposed C57BL6 mice were treated
with or without sEH inhibitor TPPU (10 mg/L, with 3-day pretreatment) for 21 days.
(**B**) Gene expression of macrophage marker *F4/80* in intestine. (**C**) Gene expression of
M2 macrophage marker *Cd163* and *Cd206* in intestine. (**D**) Immunohistochemical staining
of lysozyme in intestine (magnification 200×, scale bars: 50 μm) and quantification of
lysozyme+ cells per crypt (n = 25 crypts per group). (**E**) Gene expression of Paneth cell
marker *lysozyme* in intestine. (**F**) Gene expression of antimicrobial peptides *α-defensins-3*
in intestine. The results are expressed as mean ± SEM. n = 5-6 mice per group on gene
expression and ELISA analysis. * $P < 0.05$, ** $P < 0.01$.